Video Article

Fabrication and Operation of Acoustofluidic Devices Supporting Bulk Acoustic Standing Waves for Sheathless Focusing of Particles

C. Wyatt Shields IV[1,2], Daniela F. Cruz[1,2], Korine A. Ohiri[1,3], Benjamin B. Yellen[1,2,3], Gabriel P. Lopez[1,2,3]

[1]NSF Research Triangle Materials Research Science and Engineering Center, Duke University

[2]Department of Biomedical Engineering, Duke University

[3]Department of Mechanical Engineering and Materials Science, Duke University

Correspondence to: Gabriel P. Lopez at gabriel.lopez@duke.edu

URL: http://www.jove.com/video/53861
DOI: doi:10.3791/53861

Keywords: Engineering, Issue 109, Microfluidics, acoustophoresis, acoustofluidics, microfabrication, cellular analysis, bulk acoustic standing waves, negative acoustic contrast particles, elastomeric particles

Date Published: 3/6/2016

Citation: Shields, C.W., Cruz, D.F., Ohiri, K.A., Yellen, B.B., Lopez, G.P. Fabrication and Operation of Acoustofluidic Devices Supporting Bulk Acoustic Standing Waves for Sheathless Focusing of Particles. *J. Vis. Exp.* (109), e53861, doi:10.3791/53861 (2016).

Abstract

Acoustophoresis refers to the displacement of suspended objects in response to directional forces from sound energy. Given that the suspended objects must be smaller than the incident wavelength of sound and the width of the fluidic channels are typically tens to hundreds of micrometers across, acoustofluidic devices typically use ultrasonic waves generated from a piezoelectric transducer pulsating at high frequencies (in the megahertz range). At characteristic frequencies that depend on the geometry of the device, it is possible to induce the formation of standing waves that can focus particles along desired fluidic streamlines within a bulk flow. Here, we describe a method for the fabrication of acoustophoretic devices from common materials and clean room equipment. We show representative results for the focusing of particles with positive or negative acoustic contrast factors, which move towards the pressure nodes or antinodes of the standing waves, respectively. These devices offer enormous practical utility for precisely positioning large numbers of microscopic entities (*e.g.*, cells) in stationary or flowing fluids for applications ranging from cytometry to assembly.

Video Link

The video component of this article can be found at http://www.jove.com/video/53861/

Introduction

Acoustofluidic devices are used to exert directional forces on microscopic entities (*e.g.*, particles or cells) for their concentration, alignment, assembly, confinement or separation within quiescent fluids or laminar flowstreams.[1] Within this broad class of devices, forces can be generated from bulk acoustic standing waves, surface acoustic standing waves (SSAWs)[2] or acoustic travelling waves.[3] While we focus on the fabrication and operation of devices supporting bulk acoustic standing waves, devices supporting SSAWs have received much attention recently due to their ability to precisely manipulate cells along surfaces[4] and rapidly sort cells in continuous flow channels.[5] Devices supporting bulk acoustic standing waves, however, rearrange particles based on the mechanical vibrations of the walls of the device generated by a piezoelectric transducer, which excites the standing waves in microfluidic cavities at geometrically defined resonant frequencies. This enables the potential for generating higher pressure amplitudes compared to SSAW devices, and thus, faster acoustophoretic transport of microscopic entities.[6]

These standing waves consist of a spatially periodic set of pressure nodes and antinodes, which are fixed in position as the pressure oscillates in time. Particles respond to the standing waves by migrating to the pressure nodes or antinodes, depending on the mechanical properties of the particles relative to the fluid, and which are described by the acoustic contrast factor:

$$\Phi = \frac{5\rho_p - 2\rho_f}{2\rho_p + \rho_f} - \frac{\beta_p}{\beta_f}$$

where the variables ρ and β represent density and compressibility and the subscripts p and f represent the suspended object (*e.g.*, particle or cell) and the fluid, respectively.[7] Entities that possess a positive acoustic contrast factor (*i.e.*, ϕ >0) migrate to the pressure node(s); whereas, entities that possess a negative acoustic contrast factor (*i.e.*, ϕ <0) migrate to the pressure antinodes.[7] While the majority of synthetic materials (*e.g.*, polystyrene beads) and cells exhibit positive acoustic contrast, elastomeric particles made from silicone-based materials,[8] fatty molecules[9] or other highly elastic constituents exhibit negative acoustic contrast in water. Elastomeric particles in acoustofluidic devices can be used to isolate small molecules[10] and as means to confine synthetic particles[11] or cells[12] for the purposes of discriminate sorting.[13]

Acoustofluidic devices are usually manufactured from standard materials (*e.g.*, silicon and glass) that have sufficient rigidity to support an acoustic standing wave. In many acoustofluidic devices (including the device shown herein), the mechanical waves are designed to resonate at the lowest harmonic mode, which consists of a half-wavelength standing wave spanning the width of the microchannel. This configuration has a pressure node at the center of the channel and pressure antinodes along the peripheries of the channel. It has been shown previously that these systems can be used for chip-based cytometry applications[14-16] and applications ranging from the trapping of cells to the concentration of cells.[17,18]

We describe the process of fabrication, methods for use and representative performance capabilities of an acoustofluidic device that supports bulk acoustic standing waves. This device requires one photolithography step, one etching step and one fusing step to permanently bond a glass "lid" to the etched silicon substrate. We note that other acoustofluidic devices that support bulk acoustic standing waves can be fabricated from glass or quartz capillaries bound to piezoelectric transducers, which is described elsewhere.[19,20] Silicon-based devices offer the advantages of robustness and control over the flow channel geometry, which together allow for numerous types of processing for samples containing suspensions of particles and cells. The devices are reusable provided they are properly cleaned between uses (*i.e.*, by flushing the device with buffers and detergents).

Protocol

1. Photolithography

1. Design the photomask using an appropriate software package and submit the design to a qualified photomask printer.[21]
2. In a clean room facility, rinse a 6" single-side polished Si wafer with a steady stream of acetone (≥99.5%; see **Table 1**) followed by a steady stream of methanol (99.8%; see **Table 1**). Dry the wafer by spraying with N_2 gas and placing the wafer on a hot plate at 95 °C for 2 min.
   NOTE: The doping profile and crystal orientation of the wafers do not affect the following procedures.
3. Protect the trough outside of the spin coater (in a standard spin coat hood) by covering with a sheet of Al foil and place the clean Si wafer on the center of the vacuum chuck in the spin coater to secure the wafer.
4. Deposit positive photoresist directly onto the center of the wafer by carefully pouring until the photoresist covers most of the wafer. Take care to ensure there are no bubbles in the photoresist.
   NOTE: The exact procedures in Steps 1.5-1.10 correspond to the photoresist shown in **Table 1**; different procedures may be required for different photoresists.
5. Start the spin cycle by performing the following procedures:
   1. Program a speed of 300 rpm, a ramp of 100 rpm/sec, and a spin time of 5 sec to begin the spin cycle.
   2. Program to a speed of 1,800 rpm, a ramp of 1,000 rpm/sec, and a spin time of 60 sec to evenly spread the photoresist.
   3. Program to a speed of 0 rpm, a ramp of 1,000 rpm/sec, and a spin time of 0 sec to conclude the spin cycle.
6. Release the vacuum on the chuck and use wafer tweezers to retrieve the wafer from the chuck. Then place the wafer onto a hot plate to bake at 110 °C for 165 sec.
   NOTE: This step is referred to as the "soft bake".
7. Load the photomask into the holder of a mask aligner/photolithography machine.
8. Edit the parameters of the photolithography machine to provide an energy dosage of 1,400 mJ/cm^2 (*e.g.*, for an output intensity of 13.5 mW/cm^2, use an exposure time of #103.7 sec).
9. Remove the photopatterned wafer from the holder and place it in a solution of its corresponding developer (see **Table 1**) for 5 min.
10. Remove the wafer from the developer, wash the wafer with a steady stream of deionized H_2O and dry it with N_2 gas.
    NOTE: Over-developing may cause patterns to swell, while under-developing may cause incomplete removal of the photoresist along the photo-patterned features.
11. Inspect the wafer under a microscope to confirm the patterns printed on the photomask were transferred to the photoresist.

2. Deep Reactive Ion Etching

1. Load the photo-patterned Si wafer into the chamber of a deep reactive ion etching instrument and etch the fluidic channels into the Si wafer to the desired depth following standard etching procedures.[22]
2. Carefully unload the sample from the chamber after the etching process is complete.
3. To remove excess photoresist from the wafer, prepare a large beaker with a solution of photoresist remover (see **Table 1**) in a well-ventilated hood dedicated to solvent use and place it on a hot plate at 65 °C.
4. Submerge the wafer in the photoresist removal solution and let it soak for 1 hr.
   NOTE: Different solutions can be used to remove photoresist (*e.g.*, a solution of acetone (≥99.5%; see **Table 1**) can remove the photoresist by soaking overnight).
5. Remove the wafer from the beaker and rinse it with alternating streams of acetone (≥99.5%; see **Table 1**) and isopropyl alcohol (≥99.7%; see **Table 1**). Dry the wafer with N_2 gas.

3. Piranha Cleaning

1. In a well-ventilated hood (dedicated to the use of acids), prepare a piranha solution by adding H_2O_2 (30.0 wt.% in water; see **Table 1**) to H_2SO_4 (95.0-98.0%; see **Table 1**) to in a 1:3 ratio in a large, clean beaker.
   CAUTION: Piranha solutions are highly corrosive, are a strong oxidizer and are highly dangerous. Take extreme care in handling piranha solutions and wear the proper safety equipment.
2. Submerge the ion etched wafer with the etched-features facing up and leave for 5 min. Carefully remove the wafer and fully rinse with deionized H_2O.

3. Re-submerge the wafer in the piranha solution for 2 min. Carefully remove the wafer and fully rinse with copious deionized H_2O.
4. In a separate well-ventilated hood dedicated to solvent use, wash the wafer with a steady stream of acetone (≥99.5%; see **Table 1**) followed by a steady stream of methanol (99.8%; see **Table 1**) and dry the wafer with N_2 gas. Dispose of the piranha solution by following the appropriate safety procedures.

4. Prepare the Borosilicate Glass Lid

1. Using a scribe tool, etch straight lines into the borosilicate glass to create rectangular segments (*e.g.*, 8 x 4 cm^2). Carefully snap the glass to recover the rectangular segments.
2. Take one of these glass segments and place it on top of a printed copy of the desired design (with actual dimensions) to mark the location of the inlets and outlets on the glass with a black marker.
3. Drill the inlet and outlet holes into the borosilicate glass.
   NOTE: Proper safety equipment should be worn at all times.
   1. Fix a 1/8" drill bit into the mouth of drill press. Place the rectangular glass segment on top of an Al plate with drilled holes so that the marks on the glass are above the holes in the Al plate. Secure the glass on the Al plate with tape.
   2. Carefully lower the feed handle to start drilling small holes into the glass and continue to lower the handle until the hole is made through the glass. Once the hole is finished, remove the tape and slowly lift the glass to remove the glass powder. Place the glass powder in a beaker with water and discard using the appropriate safety procedures.
   3. Carefully dry the glass with a non-lint-producing absorbent cloth and follow the same procedures (Steps 4.3.1-4.3.2) to drill the other inlet and outlet holes.
4. Follow the same procedure (Section 3, above) to clean the rectangular glass segment with piranha solution.
   CAUTION: Piranha solutions are highly corrosive, are a strong oxidizer and are highly dangerous. Take extreme care in handling piranha solutions and wear the proper safety equipment.

5. Anodic Bonding

1. Using a scribe tool, etch straight lines into the Si wafer around the perimeter of the microfluidic chip such that it is slightly smaller than the rectangular glass segment (*e.g.*, 7 x 3 cm^2). Carefully snap the wafer along the etched lines.
2. Rinse the Si segment with a steady stream of acetone (≥99.5%; see **Table 1**) followed by a steady stream of methanol (99.8%; see **Table 1**). Place the wafer on a hot plate at 95 °C for 2 min to dry.
3. With the etched-features on the Si segment facing up, carefully add the clean glass on top of the Si segment and make sure the holes align properly.
4. Carefully flip the segments while ensuring the holes are kept aligned. Since the glass segment is larger than the Si segment, secure the two segments with double-sided tape where half of the tape secures the vertical edges of the Si segment and the other half of the tape secures the overhanging glass. Then flip the segments again such that the glass segment is on top, and place the segments on top of a metal slab on a hot plate.
5. Carefully add a second metal slab (*e.g.*, steel) of a sufficiently heavy weight (*i.e.*, at least 5 kg) directly to the top of the assembled glass and Si segments.
   NOTE: This metal slab should not be in contact with the Si segment or the conductive tape.
6. Using a high voltage power supply, connect one lead (power) to the metallic slab on top of the assembled glass and Si segments and the other lead (ground) to the bottom metallic slab.
7. Turn the voltage on the underlying hot plate to 1,000 V. Check the applied voltage by using multimeter; press one probe against the bottom plate and the other probe against the top plate.
   CAUTION: The high voltage is extremely dangerous; be careful not to touch the metallic slabs or the connecting wires.
8. Leave the hot plate at 450 °C for 2 hr to allow the glass "lid" to anodically bond to the Si substrate. Return after 2 hr to turn off the hot plate, turn off the DC power supply and remove the device from the metallic slabs.
   WARNING: The metallic slabs will be extremely hot during and after the bonding process, so allow the materials to cool for at least 1 hr after turning off the hot plate.

6. Finalizing the Acoustofluidic Device

1. Scrape the surface of the glass with a razor to remove grime produced by the anodic bonding and clean the surface of the glass with acetone.
2. Prepare a sheet of polydimethylsiloxane (PDMS) approximately 5 mm thick and cut several small, square slabs approximately 10 x 10 mm^2 (see **Table 1**).[23]
3. Use a 3 mm biopsy punch to cut one hole in the center of each PDMS slab so as to insert the silicone tubing through it. Place the slabs directly on top the holes on the glass substrate and glue the slabs with epoxy.
   NOTE: Be careful not to use too much glue as it will occlude the holes of the device.
4. Carefully glue the lead zirconate titanate (PZT) transducer to the Si segment on the back side of the device, centered-underneath the microchannel.
5. Solder two wires to the two conductive areas on the PZT transducer. Take care that the wires are securely attached to the PZT transducer. Insert the silicone tubing through the holes in the slabs of PDMS and add additional glue around slabs and the tubing to secure their attachment.

7. Operating the Acoustofluidic Device

1. Securely mount the device onto a microscope stage with the microchannel directly underneath the objective.
   NOTE: Ensure the PZT transducer does not make contact with the stage by placing a small insert underneath the device.
2. Using standardized connectors, connect the silicone tubes from the outlets of the device to syringes secured on syringe pumps.
   NOTE: This configuration is intended for "withdrawal mode"; syringe pumps may alternatively be used to inject the sample into the device.
3. Place the silicone tube leading to the inlet of the device in a vial containing the fluid sample (*e.g.*, a suspension of polystyrene beads or cells).
4. Place the vial containing the fluid sample on a stir plate to continuously mix the sample and ensure that a constant concentration of particles or cells is maintained throughout the course of the experiment.
5. Connect the wires from the PZT transducer to the output from a power amplifier in series with a function generator. Program the settings on the function generator (*e.g.*, peak-to-peak voltage and frequency) and monitor the output signal from the amplifier using an oscilloscope. Turn on the function generator and power amplifier to begin actuating the PZT transducer.[6]
   1. To estimate the resonant frequency of the device, follow the equation $c = \lambda * f$, *where* c is the speed of sound of the medium (*i.e.*, water), λ is the acoustic wavelength and f is the frequency of the PZT transducer. In the case of a half-wavelength harmonic (which we show in the Representative Results Section), the width of the microchannel should be half the length of the standing wave.
   2. Use a peak-to-peak voltage setting within the range of 0-50 V.
      NOTE: An increase in the applied voltage results in higher pressure amplitudes, and thus, more rapid acoustophoresis.
6. Turn on the microscope and ensure the microfluidic channel is clearly in focus.
7. Turn on the syringe pump to apply flow and introduce the sample into the device. Monitor the entities flowing through the device with the microscope on fluorescence mode.
8. Ensure the device efficiently focuses particles by adjusting the peak-to-peak voltage supplied to the PZT transducer to modify the pressure amplitude and by performing a frequency sweep near the expected resonant frequency to identify the empirical resonant frequency.

Representative Results

We designed the acoustofluidic device to contain a trifurcating inlet, a main channel with a width of 300 µm and a trifurcating outlet (**Figure 1A**-**B**). We note that we only used one inlet for all experiments in this study (*i.e.*, to achieve sheathless focusing of particles via acoustic radiation forces) by blocking the other inlets with removable plugs. Following the procedures described above, we constructed a chip possessing a channel width of 313 µm, with an error of #4% due to imperfections during the microfabrication process (**Figure 1C**-**D**). We operated the device at a driving frequency of 2.366 MHz to induce a half-wavelength harmonic standing wave.

We used a signal generator connected to a power amplifier to generate the high frequency sinusoidal waveform to actuate the PZT transducer. We used an oscilloscope to measure the peak-to-peak output voltage (V_{pp}) generated from the power amplifier to verify the fidelity of the signal shape and amplitude. Using a syringe pump, we first injected a suspension of green fluorescent polystyrene beads at a rate of 100 µl/min without actuation of the PZT transducer as a negative control (**Figure 2A**). Next, we actuated the device at 2.366 MHz to form a half-wavelength standing wave across the width of the microchannel (V_{pp} = 40 V; **Figure 2B**). We found that these particles, which have a positive acoustic contrast factor, focused along the pressure node as expected.[6] We also injected red fluorescent particles with a negative acoustic contrast factor (*i.e.*, $\phi \approx -0.88$, synthesized from a process described previously)[8] to verify that our device could induce their concentration along the pressure antinodes (**Figure 2C**).

Finally, we explored the extent of focusing of particles with a positive acoustic contrast factor at a range of flow rates (*i.e.*, 0 to 1,000 µl/min as regulated by a syringe pump) and voltages (*i.e.*, 0 to 50 Vpp). Videos comprised of 15 frames were collected for each condition. ImageJ software was used to sample five of the fluorescence intensity profile across the width of the microchannel. A numerical computing program was used to average the intensity profiles for each condition and to smooth the averaged data using an inline filtering program. As expected, the extent of particle focusing (*i.e.*, as defined by the width of the fluorescence peak, corresponding to the width of the stream of particles) decreased with increasing flow rates (**Figure 3A**). We also found that the extent of particle focusing increased with increasing applied voltages (**Figure 3B**).

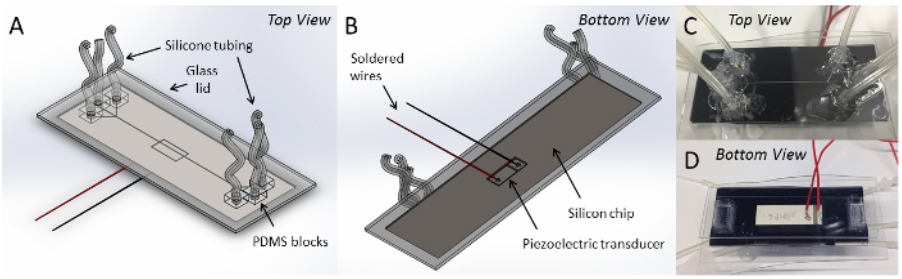

Figure 1: Acoustofluidic device supporting bulk acoustic standing waves. Schematic views of the top (**A**) and bottom (**B**) of a device comprised of an etched silicon substrate fused to a borosilicate glass "lid", polydimethylsiloxane (PDMS) blocks connected to silicone tubing and a piezoelectric transducer soldered to wires glued to the bottom of the device. Photographs of the top (**C**) and bottom (**D**) of the device are also shown. Please click here to view a larger version of this figure.

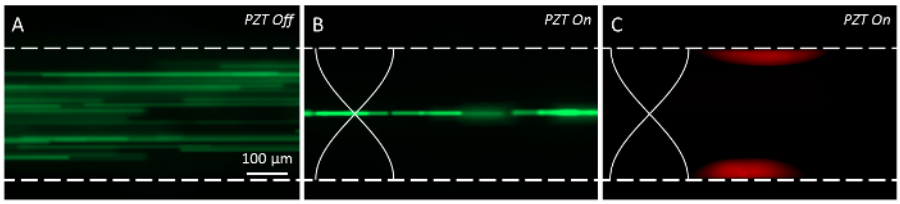

Figure 2: Acoustic focusing of particles with positive and negative acoustic contrast factors. (**A**) Prior to actuation of the lead zirconate titanate (PZT) transducer, particles with a positive acoustic contrast factor (10 µm, yellow-green polystyrene beads) flowing at 100 µl/min occupied the width of the microchannel. (**B**) After the PZT transducer is actuated (V_{pp} = 40 V and f = 2.366 MHz), the particles in (**A**) are shown to focus along the pressure node of the standing wave. (**C**) Particles with a negative acoustic contrast factor focused along the pressure antinodes of the standing wave in the absence of applied flow (V_{pp} = 40 V and f = 2.366 MHz). Please click here to view a larger version of this figure.

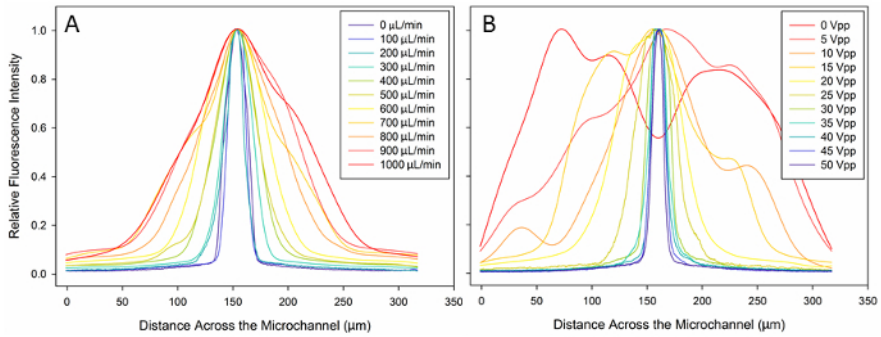

Figure 3: Focusing performance of an acoustofluidic device. Fluorescence intensity plots of polystyrene beads (shown in **Figure 2A**-**B**) are shown for (**A**) various flow rates (ranging from 0 to 1,000 µl/min) with a constant peak-to-peak voltage of 40 V and (**B**) various applied voltages (ranging from 0 to 50 Vpp) with a constant flow rate of 100 µl/min. Please click here to view a larger version of this figure.

Discussion

Acoustophoresis offers a simple and rapid approach to precisely arrange microscopic entities within fluidic microchannels without the need of sheath fluids used in hydrodynamic focusing approaches.[24] These devices provide several advantages over other methods of particle or cell manipulation (*e.g.*, magnetophoresis,[25,26] dielectrophoresis[27] or inertial forcing[28]) due to their ability to process entities without high magnetic susceptibilities, electric polarizabilities or a narrow size dispersity. Furthermore, the focusing nodes of an acoustic standing wave can be positioned far from the source of excitation, which is something that is not possible by static magnetic or electric fields as per Earnshaw's theorem.[29] An additional advantage is that acoustic devices can focus particles across a wide range of applied flow rates and independent of the flow direction, which is not possible in devices that rely on inertial forces for focusing,[28] providing the means to efficiently transport particles or cells for enhanced particle inspection for applications such as flow cytometry and particle sizing.[30,31] The ease of device fabrication and operation can directly allow for the implementation of similar devices for focusing, concentrating, fractionating and sorting objects suspended in fluids.[32]

We have shown that the primary radiation forces, which are the strongest forces produced by acoustic standing waves,[1] can focus microparticles flowing through a microfluidic channel at flow rates exceeding 10 ml/hr for a single orifice design. For a fixed flow rate of 100 µl/min, we show that our device can focus particles into a narrow streamline (*i.e.*, 50 µm across) without any sheath fluids at voltages as low as 20 V peak-to-peak, enabling a low-power method for the batchwise focusing of 10 million particles/min when processing densely concentrated solutions (*e.g.*, 6 x 10^8 particles/ml), as an example. Furthermore, this throughput can be dramatically increased by fabricating multi-orifice acoustofluidic chips or channels that are actuated with higher harmonics to produce sets of parallel nodes.[33]

While the device shown herein only requires materials and methods used in conventional microfabrication, we emphasize that there are a handful of other techniques that can be used for constructing similar devices.[19,34,35] The advantages of this approach include its simplicity as well as the durability of the final device.

The critical steps to the fabrication of these devices include photolithography to define the geometry of the microchannel, reactive ion etching to form the channel in the silicon and anodic bonding to fuse the silicon to a transparent "lid" for observation by fluorescence microscopy. All of these steps require clean room facilities to avoid the collection of dust or debris within the device. Once these steps are complete, however, bonding a PZT transducer and fluidic ports are relatively straightforward and can be performed outside of a clean room.

However, proper treatment of the device is essential for its longevity. This includes (1) incubating the device with passivating reagents (*e.g.*, poly(ethylene glycol) silane) prior to each experiment to protect the channel from residue buildup and (2) flushing the device with detergents after each experiment. Buildup of debris may compromise the fidelity of the acoustic standing wave and may reduce the ability to efficiently focus particles or cells within the device. We also note that these devices are not well-suited for highly polydisperse samples or samples containing entities approaching half of the size of the standing wave.

Acoustofluidic devices provide enormous utility for a variety of applications spanning from colloidal assembly to cell separation and flow cytometry. The ability to process biological samples with precision at high flow rates can allow for the ability of increased throughputs by these microfluidic devices, while reducing costs from superfluous reagents, large sample volumes or bulky equipment for dispensing sheath fluids. The

fabrication methods required to make acoustofluidic devices are straightforward and the procedures required for their operation are user-friendly. We hope these procedures will encourage the widespread development of similar devices to catalyze new areas of research for applications across materials science, biotechnology and medicine.

Disclosures

The authors declare that they have no competing financial interests.

Acknowledgements

This work was supported by the National Science Foundation (through grants DMR-1121107, CMMI-1363483 and Graduate Research Fellowships (GRF-1106401) to C.W.S., D.F.C. and K.A.O.) and the National Institutes of Health (R21GM111584). The authors have no conflicts of interest.

References

1. Laurell, T., Petersson, F., & Nilsson, A. Chip integrated strategies for acoustic separation and manipulation of cells and particles. *Chem Soc Rev.* **36** (3), 492-506 (2007).
2. Ding, X. *et al.* Surface acoustic wave microfluidics. *Lab Chip.* **13** (18), 3626-3649 (2013).
3. Schmid, L., Weitz, D. A., & Franke, T. Sorting drops and cells with acoustics: acoustic microfluidic fluorescence-activated cell sorter. *Lab Chip.* **14** (19), 3710-3718 (2014).
4. Guo, F. *et al.* Controlling cell-cell interactions using surface acoustic waves. *Proc Natl Acad Sci U S A.* **112** (1), 43-48 (2015).
5. Li, P. *et al.* Acoustic separation of circulating tumor cells. *Proc Natl Acad Sci U S A.* **112** (16), 4970-4975 (2015).
6. Gao, L. *et al.* Two-dimensional spatial manipulation of microparticles in continuous flows in acoustofluidic systems. *Biomicrofluidics.* **9** (1), 014105 (2015).
7. Bruus, H. Acoustofluidics 7: The acoustic radiation force on small particles. *Lab Chip.* **12** (6), 1014-1021 (2012).
8. Shields IV, C. W. *et al.* Nucleation and growth synthesis of siloxane gels to form functional, monodisperse, and acoustically programmable particles. *Angew Chem Int Ed Engl.* **53** (31), 8070-8073 (2014).
9. Petersson, F., Nilsson, A., Holm, C., Jonsson, H., & Laurell, T. Separation of lipids from blood utilizing ultrasonic standing waves in microfluidic channels. *Analyst.* **129** (10), 938-943 (2004).
10. Cushing, K. W. *et al.* Elastomeric negative acoustic contrast particles for affinity capture assays. *Anal Chem.* **85** (4), 2208-2215 (2013).
11. Johnson, L. M. *et al.* Elastomeric microparticles for acoustic mediated bioseparations. *J Nanobiotechnology.* **11,** 22 (2013).
12. Shields IV, C. W., Johnson, L. M., Gao, L., & Lopez, G. P. Elastomeric negative acoustic contrast particles for capture, acoustophoretic transport, and confinement of cells in microfluidic systems. *Langmuir.* **30** (14), 3923-3927 (2014).
13. Shields IV, C. W., Reyes, C. D., & Lopez, G. P. Microfluidic cell sorting: a review of the advances in the separation of cells from debulking to rare cell isolation. *Lab Chip.* **15**, 1230-1249 (2015).
14. Goddard, G., Martin, J. C., Graves, S. W., & Kaduchak, G. Ultrasonic particle-concentration for sheathless focusing of particles for analysis in a flow cytometer. *Cytometry A.* **69** (2), 66-74 (2006).
15. Goddard, G. R., Sanders, C. K., Martin, J. C., Kaduchak, G., & Graves, S. W. Analytical Performance of an Ultrasonic Particle Focusing Flow Cytometer. *Anal Chem.* **79** (22), 8740-8746 (2007).
16. Goddard, G., & Kaduchak, G. Ultrasonic particle concentration in a line-driven cylindrical tube. *J Acoust Soc Am.* **117** (6), 3440 (2005).
17. Lenshof, A., Magnusson, C., & Laurell, T. Acoustofluidics 8: applications of acoustophoresis in continuous flow microsystems. *Lab Chip.* **12** (7), 1210-1223 (2012).
18. Carugo, D. *et al.* A thin-reflector microfluidic resonator for continuous-flow concentration of microorganisms: a new approach to water quality analysis using acoustofluidics. *Lab Chip.* **14** (19), 3830-3842 (2014).
19. Austin Suthanthiraraj, P. P. *et al.* One-dimensional acoustic standing waves in rectangular channels for flow cytometry. *Methods.* **57** (3), 259-271 (2012).
20. Wiklund, M., Nilsson, S., & Hertz, H. M. Ultrasonic trapping in capillaries for trace-amount biomedical analysis. *J App Phys.* **90** (1), 421 (2001).
21. Shields IV, C. W. *et al.* Field-directed assembly of patchy anisotropic microparticles with defined shape. *Soft Matter.* **9** (38), 9219 (2013).
22. Yeom, J., Wu, Y., Selby, J. C., & Shannon, M. A. Maximum achievable aspect ratio in deep reactive ion etching of silicon due to aspect ratio dependent transport and the microloading effect. *J Vac Sci Technol B Microelectron Nanometer Struct Process Meas Phenom.* **23** (6), 2319 (2005).
23. McDonald, J. C., & Whitesides, G. M. Poly(dimethylsiloxane) as a material for fabricating microfluidic devices. *Acc Chem Res.* **35** (7), 491-499 (2002).
24. Golden, J. P., Justin, G. A., Nasir, M., & Ligler, F. S. Hydrodynamic focusing--a versatile tool. *Anal Bioanal Chem.* **402** (1), 325-335 (2012).
25. Hejazian, M., Li, W., & Nguyen, N. T. Lab on a chip for continuous-flow magnetic cell separation. *Lab Chip.* **15** (4), 959-970 (2015).
26. Shields IV, C. W., Livingston, C. E., Yellen, B. B., Lòpez, G. P., & Murdoch, D. M. Magnetographic array for the capture and enumeration of single cells and cell pairs. *Biomicrofluidics.* **8** (4), 041101 (2014).
27. Voldman, J. Electrical forces for microscale cell manipulation. *Annu Rev Biomed Eng.* **8** 425-454 (2006).
28. Di Carlo, D. Inertial microfluidics. *Lab Chip.* **9** (21), 3038-3046 (2009).
29. Earnshaw, S. On the nature of the molecular forces which regulate the constitution of the luminferous ether. *Trans Camb Phil Soc.* **7,** 97-112 (1842).
30. Piyasena, M. E., & Graves, S. W. The intersection of flow cytometry with microfluidics and microfabrication. *Lab Chip.* **14,** 1044-1059 (2014).
31. Grenvall, C., Antfolk, C., Bisgaard, C. Z., & Laurell, T. Two-dimensional acoustic particle focusing enables sheathless chip Coulter counter with planar electrode configuration. *Lab Chip.* **14** (24), 4629-4637 (2014).

32. Au, A. K., Lee, W., & Folch, A. Mail-order microfluidics: evaluation of stereolithography for the production of microfluidic devices. *Lab Chip.* **14** (7), 1294-1301 (2014).
33. Piyasena, M. E. *et al.* Multinode acoustic focusing for parallel flow cytometry. *Anal Chem.* **84** (4), 1831-1839 (2012).
34. Lenshof, A., Evander, M., Laurell, T., & Nilsson, J. Acoustofluidics 5: Building microfluidic acoustic resonators. *Lab Chip.* **12** (4), 684-695 (2012).
35. Evander, M., & Tenje, M. Microfluidic PMMA interfaces for rectangular glass capillaries. *J Micromech Microeng.* **24** (2), 027003 (2014).